Sauer, F. D., Blackwell, B. A., & Mahadevan, S. (1986) *Biochem. J. 235*, 453-458.
Sauer, F. D., Blackwell, B. A., & Kramer, J. K. G. (1987) *Biochem. Biophys. Res. Commun. 147*, 1021-1026.
Shaka, A. J., & Freeman, R. (1983) *J. Magn. Reson. 51*, 169-173.
Snyder, J. R., Johnston, E. R., & Serrianni, A. S. (1989) *J. Am. Chem. Soc. 111*, 2681-2687.

Structure of Chymotrypsin-Trifluoromethyl Ketone Inhibitor Complexes: Comparison of Slowly and Rapidly Equilibrating Inhibitors†

Kenneth Brady,‡ Anzhi Wei,§ Dagmar Ringe,‖ and Robert H. Abeles*,‖

Department of Toxicology, Harvard School of Public Health, 665 Huntington Avenue, Boston, Massachusetts 02115, Department of Chemistry, University of Pennsylvania, Philadelphia, Pennsylvania 19104-6323, and Graduate Department of Biochemistry, Brandeis University, 415 South Street, Waltham, Massachusetts 02254

Received December 27, 1989; Revised Manuscript Received May 2, 1990

ABSTRACT: The peptidyl trifluoromethyl ketones Ac-Phe-CF_3 (**1**) and Ac-Leu-Phe-CF_3 (**2**) are inhibitors of chymotrypsin. They differ in K_i (20 and 2 μM, respectively) as well as in their kinetics of association with chymotrypsin in that **1** is rapidly equilibrating, with an association rate too fast to be observed by steady-state techniques, while **2** is "slow binding", as defined by Morrison and Walsh [Morrison, J. F., & Walsh, C. T. (1988) *Adv. Enzymol. Relat. Areas Mol. Biol. 61*, 202], with a second-order association rate constant of 750 M^{-1} s^{-1} at pH 7.0 [Imperiali, B., & Abeles, R. (1986) *Biochemistry 25*, 3760]. The crystallographic structures of the complexes of γ-chymotrypsin with inhibitors **1** and **2** have been determined in order to establish whether structural or conformational differences can be found which account for different kinetic and thermodynamic properties of the two inhibitors. In both complexes, the active-site Ser 195 hydroxyl forms a covalent hemiketal adduct with the trifluoromethyl ketone moiety of the inhibitor. In both complexes, the trifluoromethyl group is partially immobilized, but differences are observed in the degree of interaction of fluorine atoms with the active-site His 57 imidazole ring, with amide nitrogen NH 193, and with other portions of the inhibitor molecule. The enhanced potency of Ac-Leu-Phe-CF_3 relative to Ac-Phe-CF_3 is accounted for by van der Waals interactions of the leucine side chain of the inhibitor with His 57 and Ile 99 side chains and by a hydrogen bond of the acetyl terminus with amide NH 216 of the enzyme. It is likely that the slower association rate of **2** with chymotrypsin as well as the lower K_i can be accounted for by the interaction of the P_2 (Leu) substituent. No major differences in protein conformation between the two complexes were observed. Upon dissolution of crystalline chymotrypsin-Ac-Leu-Phe-CF_3 into buffer, inhibitor is observed to dissociate from the complex at the same rate as observed for the enzyme-inhibitor complex which has been formed in solution, indicating that the complex studied crystallographically is probably identical with the complex which has been studied in solution [Imperiali, B., & Abeles, R. (1986) *Biochemistry 25*, 3760; Liang, T.-C., & Abeles, R. H. (1987) *Biochemistry 26*, 7603; Brady, K., Liang, T.-C., & Abeles, R. H. (1989) *Biochemistry 28*, 9066; K. Brady and R. H. Abeles, submitted for publication].

Peptidyl trifluoromethyl ketones are inhibitors of serine proteases. By analogy with the peptidyl aldehydes (Delbaere & Brayer, 1985; Thompson & Bauer, 1979), the nucleophilic serine of the enzyme is believed to add to the highly electrophilic trifluoromethyl ketone moiety to form a stable hemiketal adduct. Specificity and potency are provided by linking oligopeptides to the core ketone moiety in a manner analogous to improving the kinetic specificity of substrates by peptide extension (Bauer, 1978). Peptidyl trifluoromethyl ketones have been studied as inhibitors of chymotrypsin, elastase (Imperiali & Abeles, 1986; Stein et al., 1987), α-lytic protease (Govardhan, unpublished results), trypsin, and thrombin (Liang and Abeles, unpublished results) with equilibrium dissociation constants (K_i) in the micromolar to subnanomolar range.

Many peptidyl trifluoromethyl ketones are "slow-binding"[1] (Morrison & Walsh, 1988) inhibitors. Second-order rates of association (k_{on}) of peptidyl trifluoromethyl ketones with serine proteases have been measured in the range 700-80 000 M^{-1} s^{-1} (Imperiali & Abeles, 1986; Stein et al., 1987), with rates varying as a function of peptide length and composition. Slow

† Publication No. 1711 of the Graduate Department of Biochemistry, Brandeis University. This research is supported by NIH Grant GM 12633-25 to R.H.A.
* Address correspondence to this author.
‡ Harvard School of Public Health.
§ University of Pennsylvania.
‖ Brandeis University.

[1] Although the term slow binding is useful for the classification of inhibitors, it is not helpful in leading to an understanding of the mechanism of enzyme-inhibitor interaction. The association constant of enzyme and inhibitor and the dissociation constant of the enzyme-inhibitor complex are more informative. Some, but not all, slow-binding inhibitors actually have slow association constants ($\ll 10^{-7}$ M^{-1} s^{-1}). For the inhibitors under discussion, k_{on} = 700 M^{-1} s^{-1} and k_{off} = 0.0017 for **2**, and k_{on} = 3010 M^{-1} s^{-1} and k_{off} = 0.065 s^{-1} for **1** (Brady and Abeles, unpublished results).

0006-2960/90/0429-7600$02.50/0

binding to serine proteases has also been reported for the peptidyl aldehyde chymostatin (Stein & Strimpler, 1987) and peptidyl boronic acids (Kettner et al., 1988).

The basis of slow association rates of inhibitors to proteases has recently begun to be understood. Studies with phosphonamidate inhibitors of the zinc endopeptidase thermolysin (Bartlett & Marlowe, 1987) suggest that a rate-limiting displacement of a water molecule from the active site is the cause of slow association rates. A similar process may account for the slow association rates of statine-based inhibitors to the aspartyl protease renin (Kati et al., 1987). The rate of association of the peptidyl aldehyde leupeptin to papain (Schultz et al., 1989) correlates with the kinetics of ring opening of an intramolecular carbinolamine isomer of leupeptin.

Conformational change has been proposed as the cause of slow binding by peptidyl boronic acids (Kettner & Shenvi, 1984; Kettner et al., 1988), the peptidyl aldehyde chymostatin (Stein & Strimpler, 1987), and peptidyl trifluoromethyl ketones (Stein et al., 1987) to serine proteases. However, crystallographic studies of the α-lytic protease complex with a slow-binding boronic acid (Bone et al., 1987), the *Streptomyces griseus* protease B–chymostatin complex (Delbaere & Brayer, 1985), and the complex between pancreatic elastase and a tripeptidyl trifluoromethyl ketone (Takahashi et al., 1988) provide no evidence for a conformational change.

N-Acetyl-L-phenylalanyl trifluoromethyl ketone (Ac-Phe-CF_3,[2] **1**) is a rapidly equilibrating inhibitor of chymotrypsin with K_i = 20 μM. Acetyl-L-leucyl-L-phenylalanyl trifluoromethyl ketone (Ac-Leu-Phe-CF_3, **2**) is a slow-binding inhibitor with K_i = 2 μM (Imperiali & Abeles, 1986). The difference in kinetic behavior might be due to a conformational change or to significantly different modes of binding for the two inhibitors. The question of binding mode is especially pertinent because of the observation (Bachovchin et al., 1988) that peptidyl boronic acid inhibitors of α-lytic protease may form an adduct with either Ser 195 or His 57 of the enzyme, depending on the specificity of the peptidyl portion of the inhibitor. To establish such possible differences, the crystallographic structures of the chymotrypsin–**1** and chymotrypsin–**2** complexes were determined. Of particular interest are the questions whether there are major structural differences between a complex formed with a rapidly equilibrating inhibitor and a slow-binding inhibitor and whether complex formation involves conformational changes in chymotrypsin.

Materials and Methods

α-Chymotrypsin (type II, 3× crystallized), *N*-benzyl-L-tyrosine ethyl ester (BTEE), and ammonium sulfate (grade III) were obtained from Sigma Chemical Co. Cetyltrimethylammonium bromide was purchased from Aldrich Chemical Co. Other buffer salts were obtained from Fisher Scientific. The inhibitors *N*-acetyl-D,L-phenylalanyl trifluoromethyl ketone and *N*-(*N*-acetyl-L-leucyl)-D,L-phenylalanyl trifluoromethyl ketone were prepared by the method of Imperiali and Abeles (1986). Diastereomerically pure, radiolabeled Ac-L-Leu-L-Phe-CF_3 (8 mC/mmol) was a gift from Dr. T.-C. Liang.

Crystalline Enzyme–Inhibitor Complex. α-Chymotrypsin was converted to γ-chymotrypsin by the method of Corey et al. (1965). Native crystals were obtained by slowly equilibrating 250 μL of a solution containing 15 mg/mL γ-chymotrypsin, 10 mM sodium cacodylate buffer (pH 5.6), 0.75% saturated cetyltrimethylammonium bromide, and 44% saturated ammonium sulfate against 1 mL of 70–75% saturated ammonium sulfate. Crystals of 1–1.5-mm length were obtained in 1–2 weeks.

Crystals of the enzyme–inhibitor **1** complex (C–**1**) were obtained from native γ-chymotrypsin crystals by soaking them in 1 mL of a solution containing 75% saturated ammonium sulfate, 10 mM potassium phosphate, pH 7.0, 5% acetonitrile, and 2.5 mM acetyl-D,L-phenylalanine trifluoromethyl ketone. After 1 week, more inhibitor was added to bring the final concentration of inhibitor to 5.0 mM in a mother liquor containing 10% acetonitrile.

Crystals of the enzyme–inhibitor **2** complex were obtained by cocrystallization of γ-chymotrypsin according to the method described above for the native enzyme in the presence of 1 mM acetyl-L-leucyl-D,L-phenylalanine trifluoromethyl ketone.

Crystalline enzyme–inhibitor complex for kinetic studies was prepared as follows. Native crystals were soaked in 75% saturated ammonium sulfate containing 10 mM potassium phosphate, at either pH 7.0 or pH 5.6, for 4 days. Radiolabeled inhibitor **2**, *N*-[^{3}H]acetyl-L-leucyl-D,L-phenylalanine trifluoromethyl ketone, was added to a final concentration of 4 mM in the mother liquor, and the crystals were allowed to soak for 2 weeks.

Dissociation Kinetics of Crystalline Enzyme–Inhibitor Complex. The dissociation rate of the crystalline C–**2** complex was evaluated from crystals, prepared above, which had been soaked with *N*-(*N*-[^{3}H]acetyl-L-leucyl)-D,L-phenylalanyl trifluoromethyl ketone. The soaked crystals were dissolved in 200 μL of 100 mM potassium phosphate buffer (pH 7.0) at 4 °C. An aliquot of this solution was assayed with BTEE as substrate (Hummel, 1959), and the enzyme concentration was evaluated from the final velocity by use of the specific activity of fully active chymotrypsin of 1750 nmol hydrolyzed per minute per nanomole of chymotrypsin. Inhibitor content was determined from a second aliquot (50 μL) by use of a Beckman LS 1800 scintillation counter, the specific activity of the inhibitor (8 μCi/nmol), and a counting efficiency of 0.5. The remaining solution was applied to a Penefsky column (G-15, preequilibrated with the assay buffer and chilled to 4 °C; Penefsky, 1979). Aliquots of column effluent were immediately assayed for time-dependent chymotrypsin activity and for inhibitor content. The total concentration of enzyme in the solution was calculated from the fully recovered rate of BTEE hydrolysis. Dissociation constants were evaluated by using a nonlinear regression to fit the recovery curve to (Cha, 1975)

$$P(t) = P(0) + k_{cat}(E_T - E_0)\exp(-k_d t)/k_d \qquad (1)$$

where $P(t)$ = product formed at time t, E_T = total enzyme present, E_0 = active enzyme at t = 0, k_{cat} = specific activity of BTEE hydrolysis by chymotrypsin, and k_d = dissociation rate of EI complex.

Crystallographic Data Collection. Both native and inhibited crystals belong to tetragonal space group $P4_22_12$. The unit-cell dimensions (Table I) indicate that they are isomorphous with each other and that no significant changes in the structure of the unit cell have occurred as a result of complex formation.

Intensity data to 2.1-Å resolution (C–**1**) and to 1.8-Å resolution (C–**2**) were collected on a Nicolet P3 diffractometer equipped with a modified LT-1 low-temperature device. Measurements were made at −8 °C to minimize radiation damage. Data were collected with full peak scans (C–**1**) and

[2] The abbreviation Phe-CF_3 denotes the trifluoromethyl ketone analogue of phenylalanine as depicted in **1**. The complexes of chymotrypsin with inhibitors **1** and **2** are abbreviated C–**1** and C–**2**, respectively. Other abbreviations: Ac, acetyl; BTEE, *N*-benzoyl-L-tyrosine ethyl ester. References to standard peptides use nomenclature consistent with the Protein Data Bank.

Table I: Unit-Cell Dimensions and Results of Least-Squares Refinement of the Enzyme–Inhibitor Complex

	C–1	C–2	native[a]
unit-cell dimensions			
a (Å)	69.3	69.3	69.6
b (Å)	69.3	69.3	69.6
c (Å)	97.2	97.6	97.4
$\alpha = \beta = \gamma$ (deg)	90	90	90
results of the refinement			
total no. of cycles	36	38	
R ($=\sum\|F_o - F_c\|/\sum F_o$)	0.18	0.19	
no. of reflections $>1\sigma$	9255	12613	
resolution range (Å)	6–2.1	10–1.8	
no. of atoms[a]	1944	1862	
av B factor (Å^2)[b]	9.2	12.6	
final restraints applied			
σ (bond length, Å)	0.020	0.020	
σ (angle length, Å)	0.030	0.030	
σ (planar length, Å)	0.040	0.025	
deviation observed[c]			
rms Δ (bond length, Å)	0.012	0.020	
rms Δ (angle length, Å)	0.029	0.043	
rms Δ (planar length, Å)	0.032	0.052	

[a] Segal et al., 1971. [b] Non-hydrogen, including solvent. [c] These Δ values are root-mean-square (rms) deviations from the corresponding values for ideal groups derived from small-molecule structural studies (Sielecki et al., 1979).

Wyckoff scans (C–**2**; Wyckoff, 1985). Two crystals were required to complete data collection of C–**1**, and one crystal was required for C–**2**.

Data were corrected for radiation damage (Hendrickson, 1976) and for absorption (North et al., 1968) and reduced by standard methods (Krieger et al., 1974). The radiation decay corrections were evaluated from a set of five reflections chosen to be well distributed over reciprocal space, measured every 300 measurements. A linear decay model (Hendrickson, 1976) fitted the observed data and was used to correct the observed intensities. Data from the two crystals used for C–**1** were merged with a final R_{merge} ($\sum|I - I_{av}|/\sum I_{av}$) of 0.065. A total of 9225 (65% of possible reflections to 2.1 Å, C–**1**) and 12613 (57% of possible reflections to 1.8 Å, C–**2**) measurements greater than 1σ were retained.

Difference Fourier maps with $2F_o - F_c$ coefficients were calculated by use of phases and amplitudes derived from the coordinates of native γ-chymotrypsin (Cohen et al., 1981) in the Protein Data Bank (Bernstein et al., 1977). In the calculation of native phases and structure factors, the active site water molecules were omitted to provide an undistorted view of the inhibitor density. The maps showed the bound inhibitors clearly in both cases with a distinct density bridge to the Ser 195 Oγ (Figure 1). The model and electron-density maps were displayed on an Evans and Sutherland PS300 running Frodo Version 6.3. A model of the inhibitor was constructed from standard bond lengths and angles with CHEMX (Chemical Design Ltd.). The electron density for each map was sufficiently resolved to allow the unambiguous fitting of the inhibitor model structure into the density, including the bridge of density from the inhibitor to the Oγ of Ser 195 (to form a hemiketal). The carbon atom at the hemiketal position was built as an sp^3 carbon atom in the *S* stereoconfiguration since this allowed optimal fit to the observed density. The isobutyl side chain of leucine and acetamido groups of compound **2** are very similar, and no attempt was made to resolve their relative positions until later in refinement.

Crystallographic Refinement. The structures of the complexes were refined by the restrained least-squares method with the program PROLSQ (Hendrickson & Konnert, 1979). Models of the inhibitors with optimized bond lengths were prepared with CHEMX (Chemical Design Ltd.) and adapted to the PROLSQ ideal dictionary. Restraints were applied to bond lengths and planar groups (peptide bonds, carboxyl groups, and aromatic rings) during refinement. The covalent bond between inhibitor and enzyme was defined with an ideal bond length of 1.48 ± 0.40 Å. This excludes van der Waals terms between the covalently linked atoms, while the large allowed deviation prevents undue bias on the observed distance in the refined model.

For complex C–**1**, 11 cycles of positional refinement with an overall thermal parameter using data to 3.0-Å resolution were followed by 17 cycles, extending the data to 2.1-Å resolution. Examination of a map calculated from these coordinates allowed the assignment of 184 water molecules to the structure. An additional 15 cycles of refinement, including 5 cycles with individual thermal parameters, gave a final R factor of 0.18 (Table I) from a starting R factor for this refinement of 0.40.

For complex C–**2**, eight cycles of positional refinement were followed by manual adjustment of the model to determine the relative positions of the leucine side chain and *N*-acetyl group. The overall fit of these portions of the molecule was optimized by positioning the tetrahedral leucine side chain toward His 57 and the planar acetyl side chain toward the main chain of residue 216. Examination of the $2F_o - F_c$ density map identified 99 bound water molecules. Five residues (Val 9, Lys 79, Thr 151, Leu 175, and Met 192) were identified whose side chains occupy at least two distinct alternative conformations. Refinement using individual thermal parameters was continued for 31 cycles to give a final R factor of 0.19 (Table I) from an initial R factor for this refinement of 0.34.

As a test of the validity of using tetrahedral geometry at the hemiketal center of the inhibitor model, a PROLSQ ideal dictionary (Hendrickson & Konnert, 1979) was prepared with an optimized model of inhibitor **2** with *trigonal* geometry at the ketone center. The C–**2** data set and model were refined with this trigonal PROLSQ dictionary with the restraints already described. After 10 cycles of refinement the model remained in its tetrahedral configuration, supporting our visual observation that tetrahedral geometry at the ketone center is most consistent with the observed density and is not determined by model bias.

Comparison of Maps and Refined Models. Since the C–**2** data set is at a higher resolution (1.8 Å) then the C–**1** data set (2.1 Å), C–**2** maps for direct comparison were calculated from only data to 2.1 Å. Due to minor differences in the unit-cell dimensions of the C–**1** and C–**2** complexes, refined models of the two complexes showed a slight overall shift in coordinates. The program HYDRA was used to perform a least-squares alignment of all enzyme atoms, and comparison of coordinates was made between aligned models.

Results

Kinetics of the Dissolved Crystalline Complex. We performed an experiment to compare the dissociation rate of crystalline enzyme–inhibitor complex, immediately upon dissolution, with that of the complex prepared in solution. The crystals with inhibitor **2** were prepared as described under Materials and Methods. Results using crystals prepared at pH 5.6 or pH 7.0 were identical. Immediately after dissolution of the crystals, the enzyme shows approximately 25% of maximal activity, and the stoichiometry of inhibitor with enzyme is greater than 1:1. The dissolved crystals were then passed through a sizing column. This caused a 2–8-fold dilution of enzyme and reduced the inhibitor–enzyme stoichiometry to approximately 1:1. An aliquot (10 μL) of the

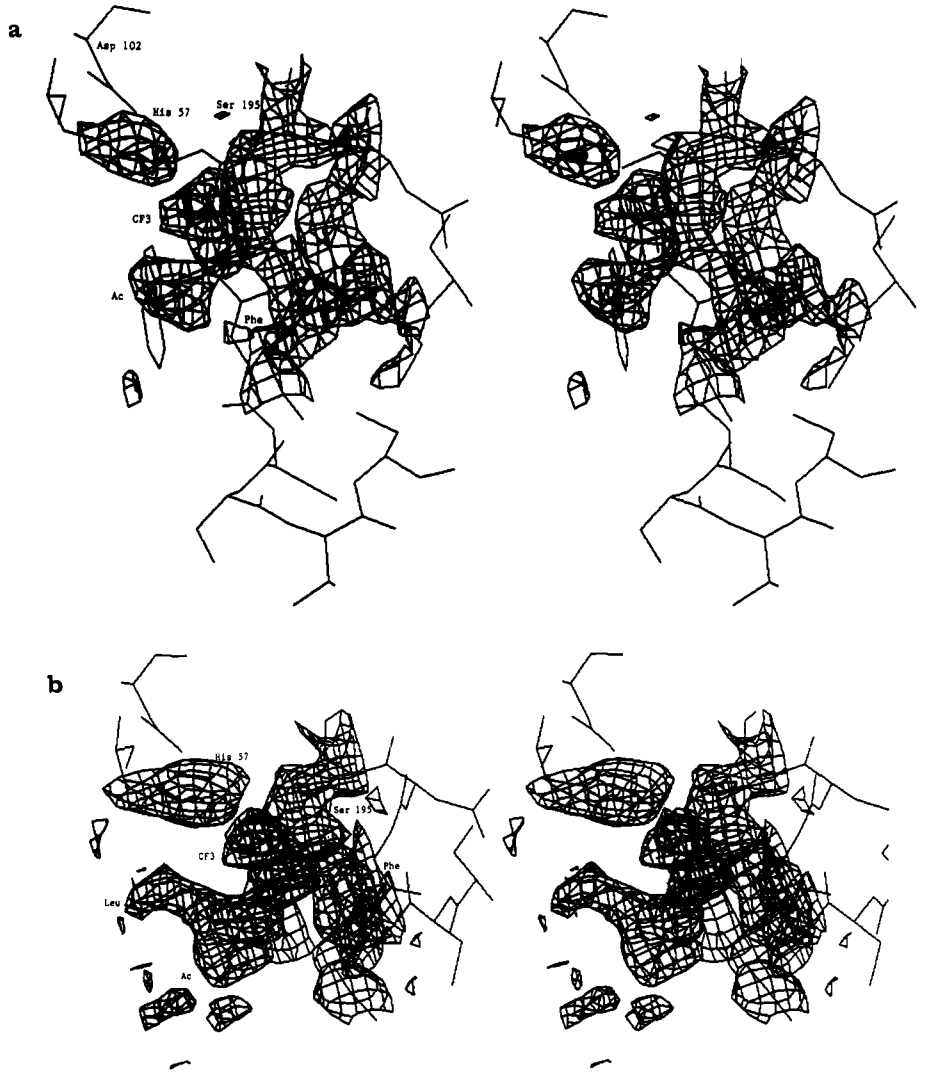

FIGURE 1: (a) Stereoview of the crystallographic density observed at the active site of the γ-chymotrypsin complex with Ac-Phe-CF_3 (C–**1**). The refined model is superimposed. The map is contoured at 1.2σ (σ = standard deviation of the map). (b) Stereoview of the crystallographic density observed at the active site of the γ-chymotrypsin complex with Ac-Leu-Phe-CF_3 (C–**2**). The refined model is superimposed. The map is contoured at 1.2σ.

solution was then added to assay buffer (1.0 mL) at 25 °C, and the initial activity remained at 25% of maximal activity. The rate of recovery to full enzyme activity was measured as 4.0×10^{-4} s^{-1}. This value is similar to that previously determined when the complex is formed in solution at pH 7.0 (9.0×10^{-4} s^{-1}; Imperiali & Abeles, 1986).

Description of the Structures of the Chymotrypsin Complexes. (1) Structural Similarities of the C–1 and C–2 Complexes. The refined model of inhibitor **1** fitted to the observed electron density for the complex between γ-chymotrypsin and **1** (C–**1**) is shown in Figures 1a and 2a. The refined model of inhibitor **2** fitted to the observed electron density for the complex between γ-chymotrypsin and **2** (C–**2**) is shown in Figures 1b and 2b. Inhibitor–enzyme contacts for both complexes are summarized schematically in Figure 3. The two structures have notable similarities and some interesting differences. Although the enzyme was treated with a racemic mixture of Ac-D,L-Phe-CF_3 and a diastereomeric mixture of Ac-L-Leu-D,L-Phe-CF_3, only the isomers with the L configuration at phenylalanine are observed on the enzyme. In both structures the electron density forms a bridge from the γ-oxygen of serine 195 to the ketone carbon atom of the inhibitor, forming a tetrahedral geometry consistent with a hemiketal covalent adduct. The refined lengths of these covalent bonds are 1.5 Å in both models. The tetrahedral ketal carbons of the inhibitors are in the *S* configuration.

The hemiketal oxygen atoms are hydrogen bonded to the amide nitrogens of Gly 193 and Ser 195 (the oxyanion hole; Robertus et al., 1972) with H-bond distances of 2.6 and 2.7 Å (see Figure 3). These models resemble previously reported structures of serine protease–inhibitor complexes (Walter & Bode, 1983; Marquart et al., 1983) in that the hydrogen bonds to the amide nitrogens of Gly 193 and Ser 195 are strong, while a hydrogen bond to the amide nitrogen of Asp 194 is weak or absent. One nitrogen (Nδ1) of the His 57 side chain and one carboxylate oxygen of Asp 102 are strongly hydrogen bonded at distances of 2.6 Å (C–**1**) and 2.5 Å (C–**2**). The other nitrogen (Nε2) of the His 57 side chain and the oxygen of Ser 195 interact weakly, if at all, at a distance of 3.2 Å in both structures.

(2) Unique Aspects of the Chymotrypsin–Ac-Leu-Phe-CF_3 (C–2) Complex. The electron density for the fluorine atoms of the trifluoromethyl group is distinct as three lobes, indicating restricted rotation about the F_3C–CO bond. Four interactions are observed that determine the orientation of the trifluoromethyl group. The dihedral angle of the F_3C–CO (trifluoromethyl–hemiketal) configuration in the refined model has a value of 58° ± 2°, so that the fluorine atoms are almost

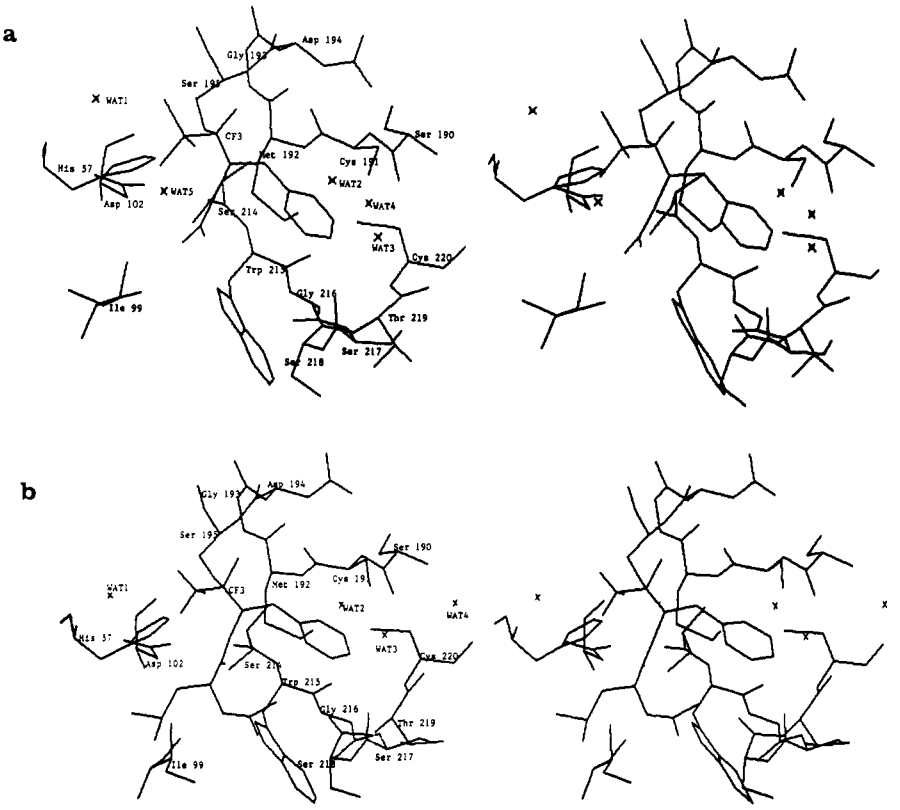

FIGURE 2: (a) Stereoview of the active site of the refined model of the complex between γ-chymotrypsin and Ac-Phe-CF_3 (C-**1**). (b) Stereoview of the active site of the refined model of the complex between γ-chymotrypsin and Ac-Leu-Phe-CF_3 (C-**2**).

perfectly staggered with respect to the ketal oxyanion. One fluorine atom interacts with the Nε2 of His 57 at a distance of 3.3 Å, representing a possible ion–dipole interaction (Murray-Rust et al., 1983). The same fluorine atom also interacts with a water molecule at a distance of 3.3 Å. A second fluorine atom points toward the amide nitrogen of Gly 193 at a distance of 3.3 Å, possibly forming a dipole–dipole interaction.

In the P_1 subsite,[3] one plane of the phenyl ring faces the side-chain and main-chain atoms of Met 192 and the Cys 191–Cys 220 disulfide bond. A water molecule lies between this face of the plane and the side-chain oxygen of Ser 189. The other face of the phenyl ring faces the main chain of residues Trp 215–Gly 216 and the acetyl terminus of the inhibitor. The large P_1 specificity pocket accommodates several solvent molecules inside the pocket, beyond the phenyl ring. One water molecule is hydrogen bonded to the carbonyl oxygen of Ser 190 and the γ-oxygen of Ser 189. Another water molecule interacts with the carbonyl oxygen of Pro 225 and the amide nitrogen of Ser 217. No specific hydrogen-bonding contacts are evident for other solvent atoms.

The P_2 leucine side chain of the inhibitor establishes close van der Waals contacts with the plane of the active site imidazole and with the side chain of Ile 99. These contacts closely resemble similar contacts at the P_2 subsite of the SGPaseA–chymostatin complex (Delbaere & Brayer, 1985) and the SGPaseA–ovomucoid third domain complex (Read et al., 1983). The N-terminal acetyl carbonyl oxygen is hydrogen bonded to the amide nitrogen (NH) of Gly 216 (2.6 Å).

[3] The nomenclature of Schechter and Berger (1967) is used to specify interactions between the protease and bound peptides. Amino acid residues of substrates are numbered P_1, P_2, etc. toward the N-terminal direction and P_1', P_2', etc. toward the C-terminal direction from the scissile bond.

*(3) Unique Aspects of the Chymotrypsin–Ac-Phe-CF_3 (C-**1**) Complex.* The electron density of the trifluoromethyl group of the C-**1** complex appears triangular, indicating that while rotation about the F_3C–CO bond is restricted, it is not as restricted as in the C-**2** complex, for which the fluorine atoms are more clearly defined by lobes of electron density. The dihedral angle for the FC–CO configuration is 57°, indicating nearly optimal staggering of the trifluoromethyl group with respect to the ketal oxyanion. One fluorine atom interacts very closely with one nitrogen (Nε2) of the His 57 side chain 2.8 Å), suggesting an ion–dipole interaction. The interaction between another fluorine atom and the amide nitrogen of Gly 193 is distant (3.5 Å). No water molecule corresponding to that which interacts with the third fluorine atom in C-**2** is observed in this structure.

In the P_1 subsite, the phenyl ring lies in the same plane as the phenyl ring of the C-**2** complex, but adjustments in the tetrahedral angles at Cα and Cβ of the inhibitor residue have resulted in a displacement of about 0.9 Å in the direction of the Met 192 side chain.

*Comparison of the C-**1** and C-**2** Complexes.* The electron density observed for the His 57 imidazole of the C-**1** complex is less planar than the density observed in the C-**2** complex, indicating relatively more disorder due to spinning of the imidazole about dthe Cβ–Cγ bond in the C-**1** complex. The density observed for the His 57 imidazole of the C-**2** complex is very flat but extends well beyond the edges of the refined imidazole ring, which is consistent with disorder due to wagging about the Cα–Cβ bond. Disorder of the imidazole in the C-**2** complex is limited by the van der Waals interactions with the Leu side chain of inhibitor **2**, and this appears strongly in the temperature factors of these atoms. The normalized temperature factor for the imidazole ring atoms ($B_{av,imidazole}/B_{av,enzyme}$) is 1.2 in the C-**1** complex and 0.4 in the C-**2** complex.

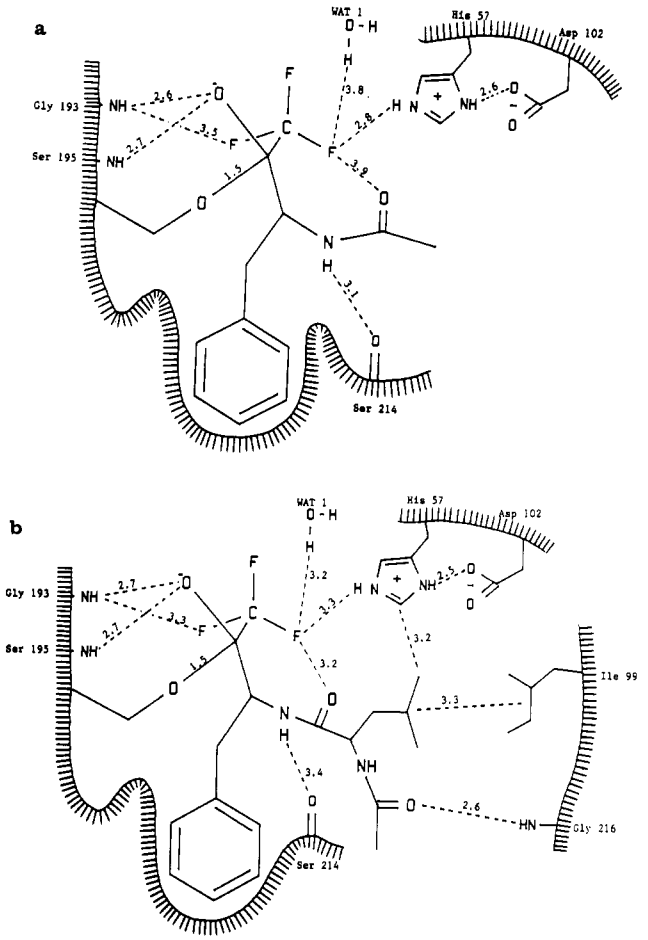

FIGURE 3: (a) Schematic diagram of the covalent, hydrogen-bonding, van der Waals, and putative dipole interactions observed in the γ-chymotrypsin–Ac-Phe-CF_3 complex. Numbers are in angstroms. Estimated rms deviation in distances is 0.2 Å. (b) Schematic diagram of the covalent, hydrogen-bonding, van der Waals, and putative dipole interactions observed in the γ-chymotrypsin–Ac-Leu-Phe-CF_3 complex. Numbers are in angstroms. Estimated rms deviation in distances is 0.2 Å.

In the refined model of the C–**1** complex, the imidazole ring of His 57 is shifted toward the CF_3 group by 0.4 Å relative to that in the C–**2** model. The carboxylate side chain of Asp 102 also shifts, so that there is little change in the imidazole–carboxylate hydrogen-bond distance between models. However, there is a significant shortening of the fluorine to nitrogen (Nε2 of His 57) distance in the C–**1** model (2.8 Å) relative to the C–**2** model (3.3 Å).

The CF_3 group, hemiketal linkage, and Cα atoms of the refined models of inhibitors **1** and **2** overlap almost exactly. A small rotation about the C–Cα bond of inhibitor **2** combined with minor adjustments in the bond angles made during refinement causes a shift of 0.3–0.9 Å in the positions of atoms of the phenyl ring of inhibitor **2** relative to **1**. This shift places the phenyl ring of inhibitor **2** more deeply into the hydrophobic pocket of the enzyme. While the phenyl ring of **2** is further away from the opening of the pocket, there is no change in the total number of average distance of nonbonded contacts between the phenyl ring and enzyme residues lining the pocket.

The P_2 (Leu) carbonyl oxygen of inhibitor **2** makes a close (3.2 Å) intramolecular contact with one fluorine atom of the trifluoromethyl group. The position of this oxygen atom is determined by the numerous van der Waals contacts with the phenyl ring on one side and with the Leu side chain and *N*-acetyl group on the other side. In the shorter inhibitor, **1**, the latter contacts are not present, and the acetyl carbonyl oxygen has rotated so as to increase the oxygen to fluorine distance to 3.9 Å.

*Comparison of the C–**1** and C–**2** Complexes to the Native*[4] *Enzyme.* The refined models of the C–**1** and C–**2** complexes were aligned to the model of native chymotrypsin (Cohen et al., 1981) by a least-squares algorithm using the program HYDRA. Following least-squares alignment, the average displacement of all main-chain atoms of both the C–**1** and C–**2** models from the native model was 0.27 Å. The His 57 imidazole ring of both inhibitor complexes is displaced by 0.4–0.5 Å away from the P_2 subsite, which, in the native enzyme and the C–**1** complex, is filled with solvent. This slight displacement is achieved via small adjustments in the main chain of His 57 and is presumably caused by steric interactions with the CF_3 groups of the inhibitors and with the P_2 Leu side chain in the C–**2** complex.

Relative to the side-chain oxygen of serine 195 (Oγ) of the native enzyme, these oxygens in both complexes have been displaced by ~0.5 Å away from the hemiketal carbon. This motion is achieved by rotation about the Cα–Cβ bond of Ser 195. There are no other significant conformational changes between native and complexed enzyme in the vicinity of the active site.

Discussion

If mechanistic conclusions concerning the basis of tight binding and slow association rates are to be drawn from crystallographic data, it is essential to know whether the crystalline complex is structurally identical with the "tight-binding" complex formed in solution. The most characteristic property of the solution complex is its slow dissociation rate. We therefore attempted to answer this question of identity between the two complexes by comparing the dissociation rate of the crystalline complex immediately upon dissolution to that of the complex formed in solution. Two limiting results can be expected: (1) the dissociation rate of the dissolved crystalline complex is more rapid than that formed in solution, indicating that the crystalline complex differs from that formed in solution; (2) the dissociation rate of the complex is the same as that formed in solution, consistent with the proposition that the two complexes are identical. We observe identical dissociation rates for the solution complex and the dissolved crystalline complex. However, this does not provide unequivocal proof for identity of the complexes. There remains the possibility that the crystalline complex is a loose-binding complex which, upon release from the restraints of the crystal structure, rapidly (more rapid than the dissociation of the inhibitor from the complex) converts to the tight-binding form. Although this interpretation appears unlikely to us, it cannot be excluded.

We have determined the three-dimensional structure of chymotrypsin in complexes with inhibitors **1** and **2**. Inhibitor **1** (Ac-Phe-CF_3) inhibits chymotrypsin with rapid equilibrating kinetics and with K_i = 20 μM. Inhibitor **2** (Ac-Leu-Phe-CF_3) shows slow-binding kinetics, with K_i = 2 μM (Imperiali & Abeles, 1986). One goal of this work was to determine whether formation of the complex of chymotrypsin with **2** involved a major conformational change of the enzyme. The results obtained here show that no major conformational change appears in the complex of either **1** or **2** with chymotrypsin and that the structures of these two complexes are very

[4] Native enzyme refers to the crystallographic model of γ-chymotrypsin described by Cohen et al. (1981). A recent report (Dixon & Matthews, 1989) indicates that native γ-chymotrypsin may contain a peptide ligand at the active site.

Table II: Selected Distances (Å) of the Catalytic Center in Transition-State and Michaelis Complexes

	Ser 195 Oγ–activated carbonyl (boron)	oxyanion hole H-bonds	Ser 195 Oγ–His 57 Nε	His 57 Nε–"leaving group" (see text)
Michaelis complexes				
(1) trypsin–PSI[a]	2.7	2.7, 3.2	2.6	4.1
(2) SGPase A–OMTKY3[b]	2.7	2.6, 3.1	2.6	3.8
transition state analogue complexes				
(3) Cht–ALPCF$_3$[c]	1.5	2.7, 2.7	3.2	3.4
(4) Cht–APCF$_3$[d]	1.5	2.6, 2.7	3.2	2.8
(5) SGPase A–chym[e]	1.6	2.9, 3.0	3.4	3.0
(6) PPE–AAPCF$_3$[f]	1.5	2.5, 2.8		3.1
(7) α-lytic–tBAPb[g]	1.7	2.6, 2.9	3.0	2.7

[a] Trypsinogen–pancreatic secretary inhibitor (M. Bolognesi et al., 1982). [b] *S. griseus* proteinase A–avian ovomucoid third domain (Read et al., 1983). [c] Chymotrypsin–Ac-Leu-Phe-CF$_3$ (this work). [d] Chymotrypsin–Ac-Phe-CF$_3$ (this work). [e] *S. griseus* proteinase A–chymostatin (Delbaere et al., 1985). [f] Porcine pancreatic elastase–AcAlaProValCF$_3$ (Takahashi et al., 1987). [g] α-Lytic protease–*t*-BOCAlaPro-boro-Val (Bone et al., 1987).

similar. The two small changes which are observed relative to native enzyme (minor changes in the average positions of the His 57 imidazole and side chain of Ser 195) are common to both the C–**1**, and C–**2** complexes. Since inhibitor **1** does not exhibit slow binding, these small changes cannot be the origins of the slow binding by inhibitor **2**. Any rate-limiting conformational adjustments which may be responsible for the slow binding of **2** relative to **1** must therefore occur at an intermediate step during the formation of the C–**2** complex, and not in the stable, tight complex which we have described.

Two binding interactions are observed in the chymotrypsin–Ac-Leu-Phe-CF$_3$ complex which are not present in the chymotrypsin–Ac-Phe-CF$_3$ complex: a hydrophobic interaction between the leucine side chain of **2** and side chains of enzyme residues 57 and 99; a well-oriented hydrogen bond between the acetyl carbonyl of **2** and the Gly 216 amide nitrogen of chymotrypsin. The sum of the binding energies of these two interactions is expected to account for the enhanced potency of Ac-Leu-Phe-CF$_3$ relative to Ac-Phe-CF$_3$ as reflected in their relative K_is. Measurements of the inhibitory potency of Ac-Leu-Phe-CF$_3$, Ac-Gly-Phe-CF$_3$, and Ac-Phe-CF$_3$ (Brady and Abeles, unpublished results) illustrate this as follows.

The hydrogen bond observed in the C–**2** complex between the terminal acetyl carbonyl and the amide NH of Gly 216 is expected to contribute 0.5–1.5 kcal/mol of stabilization energy (Fersht et al., 1985). A comparison of the inhibition constants of Ac-Phe-CF$_3$ (K_i = 20 μM) and Ac-Gly-Phe-CF$_3$ (K_i = 12 μM; Brady and Abeles, submitted for publication) agrees with this prediction: the stability of the complex with the extended inhibitor is improved 1.7-fold, corresponding to 0.3 kcal/mol of additional binding energy. We attribute this difference primarily to this hydrogen bond. The second significant set of interactions is between the leucyl side chain of inhibitor **2** and the side chains of enzyme residues His 57 and Ile 99. An estimate of the magnitude of this interaction is obtained from the comparison of the dissociation constants[5] of Ac-Gly-Phe-CF$_3$ (K_i = 12 μM) and Ac-Leu-Phe-CF$_3$ (K_i = 2 μM). The enzyme complex with the latter is 6 times more stable, corresponding to a contribution of 1 kcal/mol due to the van der Waals interactions of the isobutyl side chain. The apparent contributions of these two interactions may be compromised by the smaller structural differences observed between complexes C–**1** and C–**2**: the unfavorable fluorine–P_2 carbonyl oxygen interaction observed in the C–**2** complex, the reduced interaction between Nε of His 57 and a fluorine atom of C–**2**, and the reduced mobility of the His 57 imidazole ring of C–**2**.

The interactions unique to the slow-binding inhibitor do not seem sufficient to indicate different chemical mechanisms for the reaction of the slow-binding inhibitor and the classical inhibitor with the enzyme. The effect of the P_2 substituent of dipeptidyl trifluoromethyl ketones upon association rates with chymotrypsin is examined in more detail in Brady and Abeles (1990).

Comparisons to Other Transition State Analogue Inhibitor–Protease Complexes. The peptidyl aldehyde, boronic acid, and trifluoromethyl ketone inhibitors are all described as "transition state analogue" inhibitors (Thompson, 1973; Kettner et al., 1988; Imperiali & Abeles, 1986). Crystallographic studies are now available for each of these classes of inhibitor, and it is of interest to compare the resulting models and observe common features which characterize the putative transition state.

Table II lists the refined distances observed at the catalytic center of serine proteases in complexes with five transition state analogue inhibitors and two peptide protease inhibitors which may be more similar to a stable Michaelis complex (Huber & Bode, 1978). Several generalizations can be drawn which help define the nature of the transition state and which demonstrate the structural changes which occur during the course of catalysis by serine proteases.

In the Michaelis-type complexes (Table II, **1** and **2**) no covalent bond has formed between the Ser 195 side-chain oxygen and the scissile carbonyl, though an exceptionally close interaction has developed between these atoms. The carbonyl oxygen is positioned in the oxyanion hole so that only one strong hydrogen bond has formed with the amide NH of residue 193. A strong hydrogen bond exists between the Ser 195 side-chain hydroxyl and the His 57 imidazole Nε as the latter is poised to act in its catalytic role as a general base. Interactions of the His 57 Nε with the amide nitrogen of the P_1' (leaving group) residue are very weak (3.8 Å).

In the transition-state complexes (Table II, **3**–**7**), proton abstraction by the His 57 imidazole Nε is complete, and the Ser 195 side-chain oxygen forms a covalent bond to the activated carbonyl or boron. The change from trigonal of tetrahedral geometry at the carbonyl (boron) permits formation of two strong hydrogen bonds from the oxyanion to the amide NH's of residues 193 and 195. With the serine–histidine interaction weakened (>3 Å), the protonated His 57 imidazole Nε is free to donate its proton to the leaving group. While formal leaving groups are absent in these transition-state

[5] K_i values were measured under the following conditions: pH 7.0, 100 mM phosphate, 38 μM chymotrypsin, and 70 μM proflavin. The dissociation constants (K_i) of the chymotrypsin–inhibitor complexes obtained by procedures to be described in a subsequent publication differ slightly, but consistently, from previously reported values measured by progress-curve (Cha, 1975) techniques.

complexes, in all cases there is a moderate to strong interaction of the His 57 imidazole Nε with an analogous atom.

Conclusions

We have presented the crystallographic structures of the complexes of chymotrypsin with the rapidly equilibrating trifluoromethyl ketone inhibitor **1** and the slow-binding trifluoromethyl ketone inhibitor **2**. Interactions of both inhibitors with the catalytic triad and the oxyanion hole of chymotrypsin are similar to each other and to interactions observed in other complexes of serine proteases with transition-state analogue inhibitors. The acetylleucine terminus of inhibitor **2** makes one strong hydrogen bond and several van der Waals contacts to the enzyme, which are consistent with the 20–30-fold enhancement in the stability of the chymotrypsin complex with **2** relative to the complex with **1**. There is no evidence for a conformational change either between the chymotrypsin–**1** and chymotrypsin–**2** complexes or between complex and native γ-chymotrypsin. Therefore, the slow second-order association rate constant observed with inhibitor **2** is not due to a slow conformation change between native γ-chymotrypsin and the enzyme–inhibitor **2** complex.

Acknowledgments

We thank Nyla Spawn for assistance in preparation of the manuscript.

References

Bachovchin, W. W., Wong, W. Y. L., Farr-Jones, S., Kettner, C. A. & Shenvi, A. B. (1988) *Biochemistry 27*, 7689.

Bartlett, Paul, A., & Marlowe, Charles K. (1987) *Biochemistry 26*, 8553.

Bauer, Carl-Axel (1978) *Biochemistry 17*, 375.

Bernstein, F. C., Koetzle, T. F., Williams, G. J. B., Meyer, E. F., Jr., Brice, M. D., Rodgers, J. R., Kenard, O., Shimanouchi, T., & Tasumi, M. (1977) *J. Mol. Biol. 112*, 535.

Bolognesi, M., Gatti, G., Menegatti, E., Guarneri, M., Marquart, M., Papamokos, E., & Huber, R. (1982) *J. Mol. Biol. 162*, 839.

Bone, Roger, Shenvi, Ashok B., Kettner, Charles A., & Agard, David A. (1987) *Biochemistry 26*, 7609.

Brady, K., & Abeles, R. H. (1990) *Biochemistry* (following paper in this issue).

Brady, Kenneth, Liang, Tzyy-Chyau, & Abeles, Robert H. (1989) *Biochemistry 28*, 9066.

Cha, Sungman (1975) *Biochem. Pharmacol. 24*, 2177.

Cohen, G., Silverton, E. W., & Davies, D. R. (1981) *J. Mol. Biol. 148*, 449.

Corey, Robert B., Battfay, Olga, Bruekner, David, & Mark, Frances G. (1965) *Biochim. Biophys. Acta 94*, 535.

Delbaere, L. T. J., & Brayer, G. D. (1985) *J. Mol. Biol. 183*, 89.

Dixon, M. M., & Matthews, B. W. (1989) *Biochemistry 28*, 7033.

Fersht, Alan R., Shi, Jian-Ping, Knill-Jones, Jack, Lowe, Denise M., Wilkinson, Anthony J., Blow, David M., Brick, Peter, Carter, Paul, Waye, Mary M. Y., & Winter, Greg (1985) *Nature 314*, 235.

Hendrickson, Wayne A. (1976) *J. Mol. Biol. 106*, 889.

Hendrickson, W. A., & Konnert, J. H. (1979) in *Biomolecular Structure, Function, Conformation, and Evolution* (Srinivason, R., Ed.) Vol. I, pp 43–57, Pergamon Press, New York.

Huber, Robert, & Bode, Wolfram (1978) *Acc. Chem. Res. 11*, 114.

Hummel, B. C. W. (1959) *Can. J. Biochem. Physiol. 37*, 1393.

Imperiali, Barbara, & Abeles, Robert H. (1986) *Biochemistry 25*, 3760.

Kati, Warren M., Pals, Donald, T., & Thaisrivongs, Suvit (1987) *Biochemistry 26*, 7621.

Kettner, Charles A., & Shenvi, Ashok B. (1984) *J. Biol. Chem. 259*, 15106.

Kettner, Charles A., Bone, Roger, Agard, David A., & Bachovchin, William W. (1988) *Biochemistry 27*, 7682.

Krieger, M., Chambers, J. L., Christoph, G. G., Stroud, R. M., & Trus, B. L. (1974) *Acta Crystallogr. A30*, 740.

Liang, T.-C., & Abeles, Robert H. (1987) *Biochemistry 26*, 7603.

Marquart, J., Walter, J., Deisenhofer, J., Bode, W., & Huber, R. (1983) *Acta Crystallogr. B39*, 480.

Morrison, J. F., & Walsh, C. T. (1988) *Adv. Enzymol. Relat. Areas Mol. Biol. 61*, 202.

Murray-Rust, P., Stallings, W. S., Monti, C. T., Preston, R. K., & Glusker, J. P. (1983) *J. Am. Chem. Soc. 105*, 3206.

North, A. C. T., Phillips, D. C., & Matthews, F. S. (1968) *Acta Crystallogr. A24*, 351.

Penefsky, H. S. (1979) *Methods Enzymol. 56*, 527.

Read, R. J., Fujinaga, M., Sielecki, A. R., & James, M. N. G. (1983) *Biochemistry 22*, 4420.

Robertus, J. D., Alden, R. A., Birktoft, J. J., Kraut, J., Powers, J. C., & Wilcox, P. E. (1972) *Biochemistry 11*, 2439.

Schechter, I., & Berger, A. (1967) *Biochem. Biophys. Res. Commun. 27*, 157.

Schultz, Richard M., Varma-Nelson, P., Ortiz, Robert, Kozlowski, Karen A., Orawski, Arthur T., Pagast, Peter, & Frankfater, Allen (1989) *J. Biol. Chem. 264*, 1497.

Segal, D. M., Powers, J. C., Cohen, G. H., Davies, D. R., & Wilcox, P. E. (1971) *Biochemistry 10*, 3728.

Sielecki, A. R., Hendrickson, W. A., Broughton, C. G., Delbaere, L. T. J., Brayer, G. D., & James, M. N. G. (1979) *J. Mol. Biol. 134*, 781.

Stein, R. L., & Strimpler, A. M. (1987) *Biochemistry 26*, 2611.

Stein, R. L., Strimpler, A. M., Edwards, P. D., Lewis, J. J., Mauger, R. C., Schwartz, J. A., Stein, M. M., Trainor, D. A., Wildonger, R. A., & Zotolla, M. A. (1987) *Biochemistry 26*, 2682.

Takahashi, L. H., Radhakrishnan, R., Rosenfield, R. E., Jr., Meyer, E. F., Jr., Trainor, D. A., & Stein, M. (1988) *J. Mol. Biol. 201*, 423.

Thompson, R. C. (1973) *Biochemistry 12*, 47.

Thompson, R. C., & Bauer, C.-A. (1979) *Biochemistry 18*, 1552.

Walter, J., & Bode, W. (1983) *Hoppe-Seyler's Z. Physiol. Chem. 364*, 949.

Wyckoff, H. W. (1985) *Methods Enzymol. 114*, 330.